A simple synthesis route and characterisation of Co_3Mo_3C†

Xiao-Hui Wang,[a,b] Ming-Hui Zhang,*[a] Wei Li[a] and Ke-Yi Tao[a]

Received 4th June 2007, Accepted 21st August 2007
First published as an Advance Article on the web 30th August 2007
DOI: 10.1039/b708363g

A simple, one-step thermal decomposition method for the preparation of Co_3Mo_3C is reported in this paper. In this novel synthesis route, a mixed-salt precursor, containing $Co(CH_3COO)_2{\cdot}4H_2O$, $(HMT)_2(NH_4)_4Mo_7O_{24}{\cdot}2H_2O$ (HMT = hexamethylenetetramine), and excess HMT is directly decomposed to the bimetallic carbide under flowing argon at 1023 K. The role of HMT in the preparation process has been investigated and a detailed reaction mechanism is proposed based on the experimental results. The bimetallic carbide is characterised by X-ray diffraction, scanning electron microscopy, high-resolution transmission electron microscopy, BET surface area measurement and X-ray photoelectron spectroscopy. Furthermore, the activity of the as-prepared Co_3Mo_3C is evaluated by a 3-methylpyridine hydrodenitrogenation (HDN) reaction. The catalyst produced from this method provides better reactivity compared to the Co_3Mo_3C catalyst prepared by the conventional temperature-programmed reduction method.

Introduction

The transition metal carbides, in particular the Group VI carbides have been extensively studied due to their unique chemical and physical properties, especially their exceptional reactivity in various industrial processes. It has been proved that the structures of carbides are determined by geometry and electronic factors other than an arbitrary combination of two metals in Group IV–VI, which can compose transition bimetallic carbides. According to the literature, ternary carbides of Co–Mo,[1–4] Co–W,[5–7] Fe–Mo,[2] Nb–Mo[8,9] Nb–W,[9] Fe–W,[10] Ni–W[11] are reported to be in existence. Among these examples, the η-phase Co–Mo combination is consistent with the widely used molybdenum-based petroleum refining catalysts, and therefore, gained a lot of attention for their potential catalysis applications. In the case of Co–Mo carbide, the array of metal atoms in the cubic carbide forms the Ti_2Ni structure. Meanwhile, small electronegative non-metal carbon atoms fill the octahedral holes, which generates the η-carbide with the filled Ti_2Ni structure.[12] Although the introduction of a second metal can usually modify the structure and promote the catalytic performance of the parent metal to form multi-functional catalysts, few studies have been reported regarding the catalytic properties of the bimetallic carbides. This could be due to the severe conditions and complex steps required for the synthesis of bimetallic carbides in comparison with the monometallic ones.

Some synthetic approaches under severe conditions have been explored in the preparation of Co–Mo carbides. In 1988, $Co_6Mo_6C_2$ (Co_3Mo_3C) and Co_6Mo_6C were prepared by a two-stage reaction method with $Co(en)_2MoO_4$ as the precursor and their structures were determined by Rietveld analyses of powder neutron diffraction data.[1] Recently, the conventional method for the preparation of Co–Mo carbide was achieved through the carburization of the corresponding nitride in a hydrocarbon/H_2 flow by temperature-programmed reduction (TPR).[2,4] In the carburization of nitride, the reaction could be considered as topotactic in the sense that the structure of the metal atoms remained unaltered, while the nitrogen and carbon atoms exchanged their interstitial positions. This method had also been demonstrated to be a successful route for the preparation of Fe–Mo,[2] Nb–Mo[9] and Nb–W[9] bimetallic carbides. However, because the nitride precursor also needs to be synthesized by another TPR process under NH_3 flow, the whole process then involved two rigorous TPR stages and limited its application. Another carburization approach was presented by Xiao *et al.* who had used an oxidic precursor instead of nitride, in which it was difficult to gain a single-phase product because of the occurrence of a phase separation (cubic and hexagonal).[13] However, Nagai and Matsuda synthesized pure phase Co_3Mo_3C crystallites recently by the carburization of an oxidic precursor at 873 K and subsequently heating in hydrogen to 1123 K.[14] Besides, Liang *et al.* developed a carbothermal hydrogen reduction method for the preparation of supported Co_3Mo_3C as well as nanostructured β-Mo_2C and W_2C.[3,15,16] This novel route relies on the activated carbon material acting as support and carbon source. Thus, it is difficult to utilize this method to prepare bimetallic Co–Mo carbide loaded on other supports. It is noted that the support for molybdenum-based hydrotreating catalysts is generally metal oxide. Then, it is worthwhile to develop a simple and convenient method to prepare bulk and supported Co–Mo carbide catalysts.

Recently, an organic amine hexamethylenetetramine (HMT) has been employed as nitrogen source and reducing agent to synthesize monometallic nitride Mo_2N through the thermal decomposition of molybdate HMT complexes.[17] Previously, our group has successfully prepared Ni–Mo and Co–Mo bimetallic nitrides using this method.[18] Afanasiev had found that an analogy existed between the HMT based method and carbothermal

[a]*Institute of New Catalytic Materials Science, College of Chemistry, Nankai University, Tianjin, 300071, P. R. China. E-mail: Zhangmh@nankai.edu.cn; Fax: +86-22-23507730; Tel: +86-22-23507730*
[b]*Department of Stem Cell and Regenerative Medicine, Beijing Institute of Transfusion Medicine, Beijing, 100850, P. R. China*

† Electronic supplementary information (ESI) available: XPS spectra of Co 2p in Co_3Mo_3C before and after Ar sputtering. See DOI: 10.1039/b708363g

preparations,[17] and proposed that the formation of nitride was assisted by the reduction of oxide with carbon. Taking into account the applicability of the carbothermal reduction in the field of carbide preparation, it would be desirable to apply the HMT based method to the preparation of bimetallic carbides.

In this study, we report a successful synthesis of pure phase Co_3Mo_3C through a one-step thermal decomposition of mixed metal salt and excess HMT in flowing argon. The role of HMT in the formation process has been investigated and a formation mechanism is proposed. 3-Methylpyridine hydrodenitrogenation (HDN) was applied as a model reaction for the evaluation of the Co_3Mo_3C catalyst from this new process.

Experimental

Commercially available solvents and reagents were used for the whole process. A precursor was prepared by dissolving $Co(CH_3COO)_2{\cdot}4H_2O$ (Tianjin No. 3 Chemical Reagent Factory, China, AR grade), $(NH_4)_6Mo_7O_{24}{\cdot}4H_2O$ (Tianjin Chemical Reagent No. 1 Plant, China, AR grade) and HMT (Tianjin Chemical Reagent No. 1 Plant, AR grade) with a desired molar ratio in 15% $NH_3{\cdot}H_2O$ solution under stirring. The molar ratio of the above compounds was confirmed by trial and error with the fixed atomic ratio of Co/Mo = 1. The magenta solution was evaporated at room temperature under ambient conditions to dryness and a magenta slurry was obtained. The resulting material was dried under vacuum at 353 K for 6 h and then crushed to a fine powder. Co_3Mo_3C was synthesized by thermal decomposition of the as-prepared powder precursor in a stainless steel reactor under a flow of argon (99.99%). In the thermal treatment process, the system was heated to 1023 K with a rate of 10 K min^{-1} and the reaction mixture was held at this temperature for 2 h. After the heat treatment, the samples were cooled at a natural rate to room temperature under argon and passivated in a flow of 1 mol% O_2/N_2 for 2 h.

For comparison purposes, Co_3Mo_3C was also synthesized from Co_3Mo_3N precursor by the conventional temperature-programmed carburization method under flowing 20 mol% CH_4/H_2 mixture at a VHSV of 6000 h^{-1}. Co_3Mo_3N precursor was prepared by ammonolysis of mixed metal oxides. The temperature of the nitridation process was controlled by the following three steps: rapidly from room temperature to 623 K (at 6 K min^{-1}), slowly from 623 to 973 K (at 1 K min^{-1}), and then holding at 973 K for 2 h. The system was cooled in flowing NH_3 and passivated as described above. Before carburization, the intermediate Co_3Mo_3N was reduced under H_2 flow at 673 K for 3 h to remove the passivation layer. Sebsequently, the system was heated to 923 K at the ramping rate of 5 K min^{-1} under carburizing agent CH_4/H_2, and then cooled and passivated in 1 mol% O_2/N_2 for 2 h.

The X-ray diffraction (XRD) patterns of the samples were measured at room temperature using a Rigaku D/max-2500 powder diffractometer, with Cu-Kα radiation (40 kV, 40 mA). The powder samples were mounted on a silicon plate for X-ray measurement. The carbon, nitrogen contents of the samples were determined with an Elementar Vario EL elemental analyzer. The particle size and morphology of the samples were characterised using an LEO 1530VP scanning electron microscopy (SEM). The samples were covered by a thin film of gold for better image definition. A JEM-2010FEF high-resolution transmission electron microscope (HRTEM) equipped with an EDX system (EDAX) operating at 200 kV was used to observe the morphology and microstructure of the bulk samples. The samples were dispersed in ethanol and were treated with ultrasound for 5 min and then were placed on a copper grid coated with holey carbon. The EDX signals of the carbide particles were obtained by focusing the electron beam on the particles and accumulating the spectra. When it was no longer possible to detect a clear increase in the Co and Mo peaks, the EDX counting was stopped and the spectrum stored. BET surface areas of the samples were determined from N_2 BET isotherms by Surface Area and Pore Analyzer (Quantachrome NOVA 2000e) apparatus. X-Ray photoelectron spectroscopy (XPS) characterisation was used to obtain detailed chemical analysis of the surface electrical properties from charging studies. XPS experiments were carried out with a Kratos Axis Ultra DLD spectrometer employing a monochromated Al-Kα X-ray source, hybrid (magnetic/electrostatic) optics and a multi-channel plate and delay line detector (DLD). To reduce the influence of surface oxygen, argon sputtering for 10 min was performed to remove the surface passivation layer, which did not have any effect on the surface analyses of the elements in the carbide. As an example, the spectra of Co 2p before and after sputtering is given in the ESI.†

The HDN reaction of 3-methylpyridine (Alfa Aesar, 99%) was performed in a tubular fixed-bed reactor under 3.0 MPa of H_2 at 543 K, 563 K, 583 K and 603 K. Firstly, 0.75 g of the bulk carbide samples was pressed, sieved to a final size of 20–40 mesh and diluted with quartz sand to 5.0 ml. Prior to evaluation, the catalyst was pretreated under flowing H_2 at 673 K for 3 h at atmospheric pressure. While the reactor was cooled to 523 K, a cyclohexane solution of 3-methylpyridine (1.5 wt%) was fed into the reactor by a high-pressure pump and the system was stabilized at this temperature for 5 h. The H_2 flow rate and the liquid feed rate were maintained at 50 ml min^{-1} and 5.0 ml h^{-1}, respectively. The liquid product was collected and analyzed by gas chromatography. The HDN activity was calculated by the conversion of 3-methylpyridine.

Results and discussion

The XRD patterns of Co_3Mo_3C and a series of intermediates in the thermal decomposition process are shown in Fig. 1. For comparison, the XRD pattern of Co_3Mo_3C prepared by carburization of Co_3Mo_3N precursor is also given and labeled as TPR. The temperatures listed in Fig. 1A mean the point that the heating process will be stopped as soon as it reaches the designated temperature, while the time values listed in Fig. 1B mean the period of holding the heating process at the target temperature 1023 K. As shown in Fig. 1B, there is little difference between the patterns labeled as 2 h and TPR. Moreover, all the diffraction peaks denoted for the 2 h sample agree quite well with the crystallographic planes data (JCPDS card No. 80-0339). Additionally, the BET surface areas of the two samples are close to each other, which are 14.61 $m^2\ g^{-1}$ for Co_3Mo_3C prepared by the new method and 10.03 $m^2\ g^{-1}$ for the TPR method. These results indicate that the simple thermal decomposition method is as effective as the conventional TPR method for the preparation of Co_3Mo_3C.

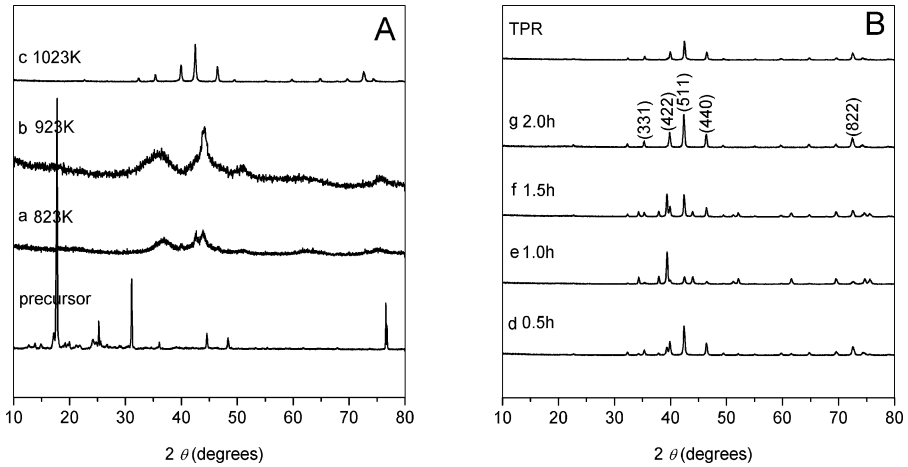

Fig. 1 XRD patterns of Co_3Mo_3C and a series of intermediates.

Fig. 2 shows typical carbon, nitrogen content corresponding to the intermediates in Fig. 1. In the overall thermal decomposition process, C, N content decreases with increasing temperature and extended holding time. A significant decrease in C and N elemental content takes place in the period of increasing the temperature. When it reaches the target temperature 1023 K, the C, N content decreases to 3.60 wt% and 1.64 wt%, respectively. With the holding time prolonged, the N content decreases close to zero, while the reduction of C content slows. In the case of Fig. 2g, the C content of the as-prepared Co_3Mo_3C sample achieves 2.39 wt%, only slightly lower than the theoretical value, which suggests its composition accords well with the molecular formula.

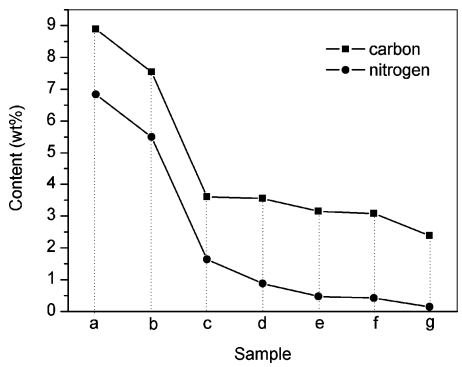

Fig. 2 Weight percentage of carbon and nitrogen in the formation process.

In order to further access the role of HMT during the formation of Co_3Mo_3C, a series of precursors with different molar ratios of $Co(CH_3COO)_2$ and HMT were prepared in parallel and all treated at 1023 K for 2 h under argon flow. The XRD patterns of the products are given in Fig. 3. To our knowledge, molybdate and HMT form the stoichiometric composition of $(HMT)_2(NH_4)_4Mo_7O_{24}{\cdot}2H_2O$ in the decomposition precursor,[17] which has been documented to be the crucial factor in the formation of monometallic and bimetallic nitrides. So in the parallel experiments, the molar ratio of $(NH_4)_6Mo_7O_{24}{\cdot}4H_2O$ and HMT was fixed at 1/2. When the molar ratio of $Co(CH_3COO)_2$ and HMT is 1 : 3, the most intense peak of the product locating at 42.70° is assigned to the formation of Co_3Mo_3N.[4] Besides, its lattice parameter is determined to be $a = 11.0173$ Å,

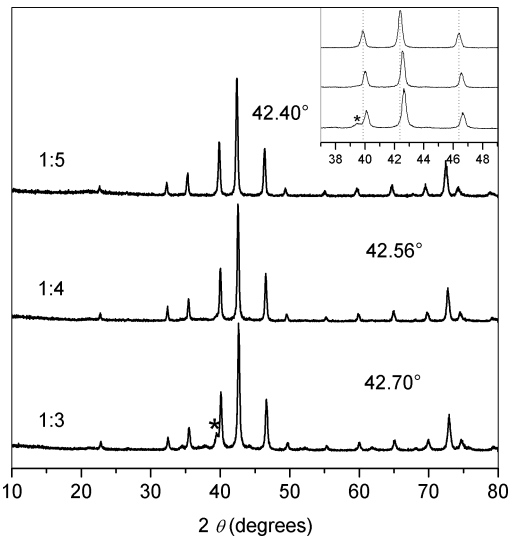

Fig. 3 The XRD patterns of the samples prepared from the precursors with different $Co(CH_3COO)_2$ and HMT molar ratios. The inset corresponds to the magnified portion. The asterisk denotes the β-Mo_2C impurity.

close to the value of Co_3Mo_3N ($a = 11.02396$ Å) according to the literature.[19] Simultaneously, the β-Mo_2C impurity is also presented, which is denoted with an asterisk. For the product marked as 1 : 4, the high HMT content makes the most intense peak shift to 42.56°. It can be ascribed to the diffraction of Co–Mo carbonitride $Co_3Mo_3C_xN_y$,[4] the chemical composition of which is $Co_3Mo_3C_{0.56}N_{0.47}$ based on carbon and nitrogen elemental analysis results. In the case of the product marked as 1 : 5, a small shift of all the peaks is observed relative to those for the 1 : 4 sample, as indicated for the three most intense peaks in the inset. In addition, there is no evidence of impurity phases according to the XRD result of the 1 : 5 pattern, suggesting the formation of single phase Co_3Mo_3C. The XRD patterns of these main products are nearly identical, reflecting the fact that they have the same metal atom arrangement and type of crystal lattice (*Fd*3*m*). To clarify the difference in microstructure between them, lattice parameters of samples 1 : 4 and 1 : 5 are calculated and confirmed to be $a = 11.0337$Å and 11.0739 Å respectively. It is worth noting that

the lattice parameter of sample 1 : 5 matches quite well with the reported value of Co_3Mo_3C ($a = 11.0709$ Å),[1] providing further evidence that the product is phase pure. Moreover, the lattice parameter of the 1 : 4 sample is between samples 1 : 3 and 1 : 5, consistent with our deduction that it is a carbonitride phase.

On the basis of the above analysis, we believe it is reasonable to assume the excess HMT to be the carbon source that makes the replacement of nitrogen with carbon take place. The overall process can be shown by the following two topotactic reactions:

$$Co_3Mo_3N + C^* \rightarrow Co_3Mo_3C_xN_y$$

$$Co_3Mo_3C_xN_y + C^* \rightarrow Co_3Mo_3C$$

C* means the active atomic carbon, which is proved to be essential for the carburization process. Herein, the C* comes from the thermal decomposition of the excess HMT, which is the so-called pyrolytic carbon.

Returning to the intermediates in Fig. 1, the formation process of Co_3Mo_3C in our new method can be described as a sequence of the following four stages. The first one is the production of amorphous γ-Mo_2N and Co metal at 923 K, as shown in Fig. 1A. In this stage, the formation of γ-Mo_2N is believed to go through the following reaction according to published results:[17]

$$(HMT)_2(NH_4)_4Mo_7O_{24}\cdot 2H_2O \rightarrow 12CO + 14H_2O + 5.33NH_3 + 1.583N_2 + 3.5Mo_2N$$

while the Co metal is mainly from the decomposition of its acetate under a reductive atmosphere, such as CO. The second stage is the presence of $Co_3Mo_3C_xN_y$ as the intermediate at 1023 K, the most intense peak of which locates at 42.48°.[4] Then, the carburization of the intermediate and the phase separation of β-Mo_2C and highly dispersed Co occur simultaneously. Apparently, the carburizing agent of this stage is the pyrolytic carbon formed by the decomposition of excess HMT, which still remains in the solid product with a content of *ca.* 3.50 wt%. In the last step, β-Mo_2C and Co are in intimate contact on a molecular basis and a solid–solid reaction between them completes the formation of the phase pure Co_3Mo_3C. At the same time, the contents of the maintained carbon and nitrogen elements in the final product decrease to the values expected.

Based on the above analysis, two key factors on preparing bimetallic carbide by this one-step method can be proposed. One is to control the content of HMT in the precursor, the other is to make the transition metal atoms presumably remain intimately mixed on a molecular or atomic level. The proper HMT content provides sufficient pyrolytic carbon, which should be transformed to atomic carbon and then inset into the lattice of the early formed bimetallic nitride. Meanwhile, the formation of bimetallic nitride relies on the latter factor. In other words, special attention has been paid to the above two significant factors so that bimetallic carbide is allowed to be obtained by this one-step synthesis. Furthermore, due to the formation of a homogeneous solution in the preparation of the precursor, this simple method has the potential to be a general route to prepare Co_3Mo_3C catalyst supported on various carriers by the impregnation method.

Shown in Fig. 4 is the SEM image of the as-prepared Co_3Mo_3C sample. The particle sizes measured by SEM are denoted in the figure. In this image, Co_3Mo_3C presents as spherical particles

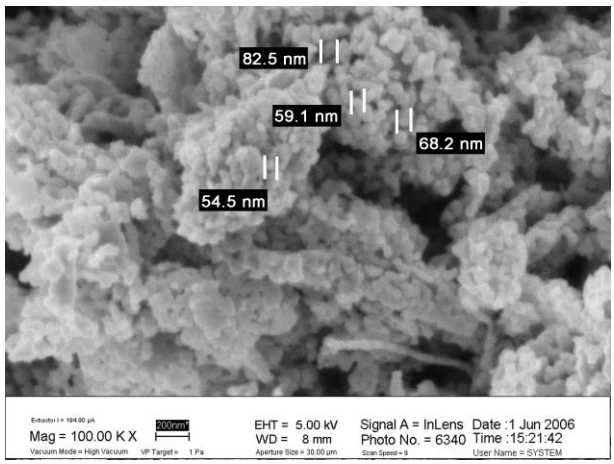

Fig. 4 SEM image of as-prepared Co_3Mo_3C.

with a size of about 55–80 nm, accumulating on a matrix of large sandwich agglomerates. Returning to the XRD pattern of Co_3Mo_3C, the average crystallite size of 45.7 nm is calculated by the Scherrer equation according to the full-width at half-maximum (fwhm) of the peak at 42.40°. This crystallite size is smaller than that estimated by SEM, which suggests that a majority of the present particles in the SEM image are not single crystals. The HRTEM micrograph together with the EDX analysis of the as-prepared Co_3Mo_3C sample is given in Fig. 5. Consistent with the XRD results, there is no evidence of impurity phases in the presented micrograph, as well as other microregions observed by HRTEM. As shown, *d*-spacing values of 0.639 nm and 0.391 nm respectively corresponding to the (111) and (220) crystallographic planes are yielded, which are in good agreement with the standard XRD data of Co_3Mo_3C (JCPDS card No. 80-0339). EDX analysis of this microregion indicates the presence of only Co, Mo, C and O elements and gives a Co/Mo molar ratio of 0.94. As the unavoidable oxygen element can be ascribed to the passivation process, the results are approximately consistent with expectation.

XPS measurement is used to investigate the chemical states of the components and the interplay of molybdenum or cobalt atoms and carbon atoms in the Co-Mo bimetallic carbide. The XPS peaks are deconvoluted using asymmetric Gaussian–Lorentzian mixed functions and a Shirley background is subtracted. The Mo 3d, C 1s and Co 2p spectra for the bulk sample are shown in Fig. 6. Fitting to the raw data in Fig. 6(a) reveals the presence of two species of Mo, one at the binding energy of 228.0 eV (Mo $3d_{5/2}$) and 231.2 eV (Mo $3d_{3/2}$), the other at 228.7 eV (Mo $3d_{5/2}$) and 232.0 eV (Mo $3d_{3/2}$). The dominant species is carbidic Mo at a mean binding energy of 228.0 eV which agrees quite well with the data in the literature.[20–23] For monometallic molybdenum carbide, Chen has observed through EXAFS that the charge of Mo is +0.2.[24] Due to the difficulty in deconvoluting $Mo^{0.2+}$ from XPS, the Mo 3d peak was deconvoluted into mostly Mo^0 with varying amounts of Mo^{2+},[25] namely Mo^{0-2+}. Thus, according to the XPS results, in the case of Co–Mo bimetallic carbide, the interstitial cobalt atoms do not bring any additional electron transfer between the molybdenum and carbon atoms. Another Mo species appearing at the binding energy of 228.7 eV (Mo $3d_{5/2}$), between the two values of 228.2 eV (Mo^{2+}) and 229.9 eV (Mo^{4+}),[25] is believed to correspond to the oxidation state of $Mo^{\delta+}$ ($2 < \delta < 4$),[25] which

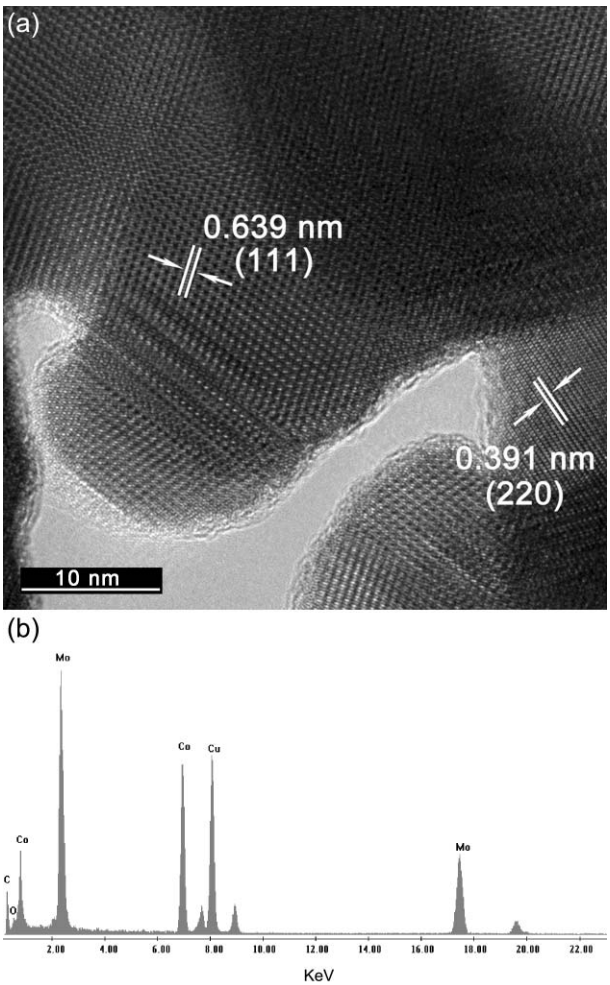

Fig. 5 HRTEM micrograph (a) of as-prepared Co_3Mo_3C together with the EDX analysis (b) of this microregion.

should come from the surface oxidation of carbidic Mo in the passivation process.

Two types of carbon peak are detected in Fig. 6(b). The C 1s spectrum presents a main peak at around 284.8 eV, attributed to the graphitic carbon[22,26] enriching the surface. The second component at 283.3 eV in Fig.6(b) can be assigned to carbon from the carbide phase.[22,26] Likewise, in the case of the Co 2p spectra in Fig. 6(c), two species of Co are present. One locates at 778.5 eV (Co $2p_{3/2}$) and the other at 781.0 eV (Co $2p_{3/2}$). Wang *et al.* proposed that in Co–C nanocomposite films, the binding energies of Co 2p in pure cobalt and cobalt carbides coincided with each other.[27] It seems that a similar result has been obtained in the current work. Unfortunately, because of low stability, more convincing experimental data for cobalt carbide is lacking. However, the structural model proposed by Prior and Battle[12] for η-carbide provides a possible interpretation for this phenomenon. In the η-carbide $[M^{32e}{}_2M^{16d}]T_3X$, M atoms locating on the 32e Wyckoff positions form tetrahedra which are capped over each face by other M atoms (16d position) to form supertetrahedra. And groups of four T_6X octahedra share vertices to form tetrahedral clusters which are vertex-linked. Consequently, the network of M atoms may be metal-like in nature corresponding to Co in our study, while the network of T atoms is more ionic, as discussed for the carbidic Mo phase in forming Mo–C bonds. That is maybe the reason why the carbidic cobalt in bimetallic carbide shows almost no shift in binding energy in comparison with metallic Co.[28,29] Such metal-like Co atoms in Co_3Mo_3C must be capable of adsorbing gaseous H_2 and activating the adsorbed H_2, which implies the outstanding hydrogenation properties of the Co–Mo carbide catalyst. On the other hand, the oxidation state of Co, giving rise to the peak centered at higher binding energy, results from the surface oxidation of Co during passivation.

In order to extend this approach to the preparation of catalysts, the activity of as-prepared bulk Co_3Mo_3C catalyst was evaluated by 3-methylpyridine HDN comparing with Co_3Mo_3C prepared by the conventional TPR method. The catalysts are denoted as Co_3Mo_3C-HMT and Co_3Mo_3C-TPR, respectively. The results of the catalytic measurements performed at different temperatures are plotted in Fig. 7. Based on the data, the activity of sample Co_3Mo_3C-HMT is slightly higher than that of sample Co_3Mo_3C-TPR at each temperature. Considering the same nature of the active component in both samples, namely Co_3Mo_3C, it may be due to a superior microstructure. Similar results have been obtained in our previous report on the activity comparison between the traditional TPR and thermal decomposition method.[30] The HMT-based method leads to higher surface areas and larger pore volumes, which improves the activity of the supported catalyst produced from the new method, despite the fact that the two catalysts possess the same active phase β-Mo_2C. In the current study, if taking the BET surface areas into consideration, the

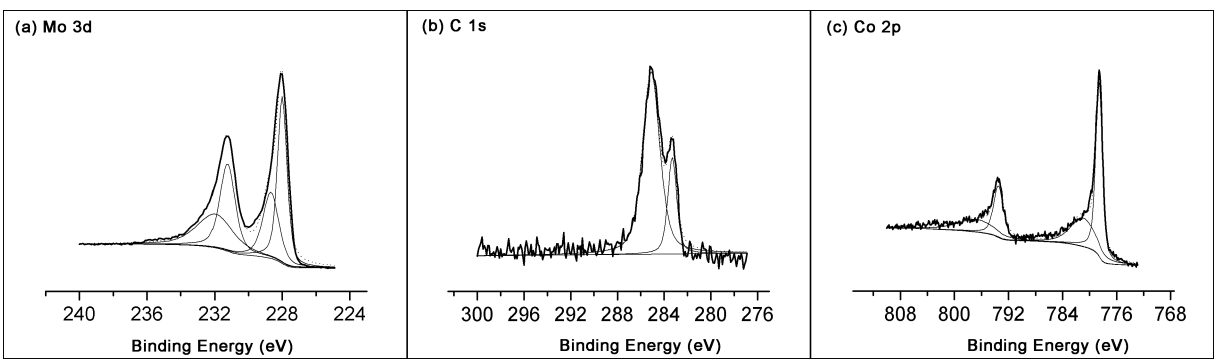

Fig. 6 XPS spectra of Mo 3d (a), C 1s (b) and Co 2p (c) of Co_3Mo_3C. Thick curves represent the raw data, thin curves represent the results of deconvolution of the spectrum into Lorentzian-broadened Gaussian peaks, and dotted curves represent the resulting fit to the raw data.

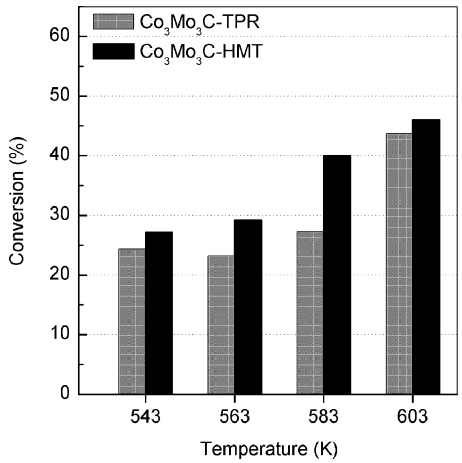

Fig. 7 The 3-methylpyridine hydrodenitrogenation activities for Co_3Mo_3C catalysts prepared by the two methods.

activity referred to unit surface area slightly decreases with the increasing surface area, but the sum of active sites of Co_3Mo_3C-HMT increases in comparison with Co_3Mo_3C-TPR. Then, it can be concluded that the high surface area has improved the dispersion of the active sites and made more metal components available. In other words, this one-step synthesis route possesses the potential to be a general approach for the preparation of Co–Mo bimetallic carbide catalysts. Research aimed at extending this approach to the preparation of other bimetallic molybdenum carbides, as well as fully exploring the formation mechanism of various transition bimetallic carbides, is currently in progress.

Conclusion

In this paper, Co_3Mo_3C is successfully prepared by the thermal decomposition of excess HMT contained in a mixed-salt precursor, in which HMT acts as both molybdate ion ligand, carbon source and reducing agent. Investigation of the formation process indicates that the transition metallic salts are intimately mixed on a molecular basis, which ensures the formation of Co_3Mo_3N. The inner carburizing agent which is generated from the decomposition of the excess HMT reacts with the bimetallic nitride, which leads to the formation of Co_3Mo_3C. Detailed analysis of the XPS characterisation shows the nearly metallic character of Co in Co–Mo bimetallic carbides. Furthermore, the interstitial cobalt atoms do not bring any additional electron transfer between molybdenum and carbon atoms in comparison with the Mo–C bonding in monometallic molybdenum carbide based on the XPS results. The HDN activity of as-prepared Co_3Mo_3C is superior to that prepared by the conventional TPR method, which proved this simple approach to be an effective method to prepare Co_3Mo_3C catalysts.

Acknowledgements

The authors are thankful for the financial support of the National Natural Science Foundation of China (Grants 20403009), the Key Project of Chinese Ministry of Education (No. 105045), and Open Foundation of State Key Laboratory of Heavy Oil Processing.

References

1 J. M. Newsam, A. J. Jacobson, L. E. Mccandlish and R. S. Polizzotti, *J. Solid State Chem.*, 1988, **75**, 296.
2 S. Alconchel, F. Sapiña and E. Martínez, *Dalton Trans.*, 2004, 2463.
3 C. Liang, W. Ma, Z. Feng and C. Li, *Carbon*, 2003, **41**, 1833.
4 S. Korlann, B. Diaz and M. E. Bussell, *Chem. Mater.*, 2002, **14**, 4049.
5 M. V. Iyer, L. P. Norcio, E. L. Kugler and D. B. Dadyburjor, *Ind. Eng. Chem. Res.*, 2003, **42**, 2712.
6 H. Shao, E. L. Kugler, W. Ma and D. B. Dadyburjor, *Ind. Eng. Chem. Res.*, 2005, **44**, 4914.
7 Z. G. Ban and L. L. Shaw, *Acta Mater.*, 2001, **49**, 2933.
8 V. Schwartz and S. T. Oyama, *J. Phys. Chem. B*, 2000, **104**, 8800.
9 J. B. Claridge, A. P. E. York, A. J. Brungs and M. L. H. Green, *Chem. Mater.*, 2000, **12**, 132.
10 D. S. Bem, C. P. Gibson and H.-C. z. Loye, *Chem. Mater.*, 1993, **5**, 397.
11 T. Xiao, H. Wang, A. P. E. York, V. C. Williams and M. L. H. Green, *J. Catal.*, 2002, **209**, 318.
12 T. J. Prior and P. D. Battle, *J. Mater. Chem.*, 2004, **14**, 3001.
13 T.-C. Xiao, A. P. E. York, H. Al-Megren, C. V. Williams, H.-T. Wang and M. L. H. Green, *J. Catal.*, 2001, **202**, 100.
14 M. Nagai and K. Matsuda, *J. Catal.*, 2006, **238**, 489.
15 C. Liang, P. Ying and C. Li, *Chem. Mater.*, 2002, **14**, 3148.
16 C. Liang, F. Tian, Z. Li, Z. Feng, Z. Wei and C. Li, *Chem. Mater.*, 2003, **15**, 4846.
17 P. Afanasiev, *Inorg. Chem.*, 2002, **41**, 5317.
18 H. Wang, W. Li and M. Zhang, *Chem. Mater.*, 2005, **17**, 3262.
19 S. Alconchel, F. Sapiña, D. Beltrán and A. Beltrán, *J. Mater. Chem.*, 1998, **8**, 1901.
20 F. Solymosi, J. Cserényi, A. Szöke, T. Bánsági and A. Oszkó, *J. Catal.*, 1997, **165**, 150.
21 D. Wang, J. H. Lunsford and M. P. Rosynek, *J. Catal.*, 1997, **169**, 347.
22 J.-M. Manoli, P. D. Costa, M. Brun, M. Vrinat, F. Maugé and C. Potvin, *J. Catal.*, 2004, **221**, 365.
23 L. Óvári, J. Kiss, A. P. Farkas and F. Solymosi, *J. Phys. Chem. B*, 2005, **109**, 4638.
24 J. G. Chen, *Chem. Rev.*, 1996, **96**, 1477.
25 K. Oshikawa, M. Nagai and S. Omi, *J. Phys. Chem. B*, 2001, **105**, 9124.
26 S. Shanmugam, D. S. Jacob and A. Gedanken, *J. Phys. Chem. B*, 2005, **109**, 19056.
27 H. Wang, S. P. Wong, W. Y. Cheung, N. Ke, G. H. Wen, X. X. Zhang and R. W. M. Kwok, *J. Appl. Phys.*, 2000, **88**, 4919.
28 A. B. Mandale, S. Badrinarayanan, S. K. Date and A. P. B. Sinha, *J. Electron Spectrosc. Relat. Phenom.*, 1984, **33**, 61.
29 A. Borgna, B. G. Anderson, A. M. Saib, H. Bluhm, M Hävecker, A. Knop-Gericke, A. E. T. Kuiper, Y. Tamminga and J. W. Niemantsverdriet, *J. Phys. Chem. B*, 2004, **108**, 17905.
30 H.-M. Wang, X.-H. Wang, M.-H. Zhang, X.-Y. Du, W. Li and K.-Y. Tao, *Chem. Mater.*, 2007, **19**, 1801.

